FEBS Letters 393 (1996) 280–286 FEBS 17519

Structural comparison of a 15 residue peptide from the V3 loop of HIV-1_{IIIb} and an O-glycosylated analogue

Xiaolin Huang[a], M. Charles Smith[b], Jay A. Berzofsky[b], Joseph J. Barchi Jr.[a,*]

[a] *Laboratory of Medicinal Chemistry, Division of Basic Sciences, National Cancer Institute, National Institutes of Health, Bethesda, MD 20892, USA*
[b] *Molecular Immunogenetics and Vaccine Research Section, Division of Basic Sciences, National Cancer Institute, National Institutes of Health, Bethesda, MD 20892, USA*

Received 7 June 1996

Abstract **As part of a program to study the effect of glycosylation on the three-dimensional structures of HIV-1_{IIIB} V3 peptide constructs, we have examined the solution structures of a 15 residue peptide (RIQRGPGRAFVTIGK, $P18_{IIIB}$), originally mapped as an epitope recognized by $CD8^+$ D^d class I MHC-restricted murine cytotoxic T-lymphocytes (CTL), and an analogue ($P18_{IIIB}$-g), O-glycosylated with an α-galactosamine on Thr-12, using NMR, circular dichroism and molecular modeling methods. Our studies show that the peptides sample mainly random conformations in aqueous solution near 25°C and become more ordered by the addition of trifluoroethanol. Upon decreasing the temperature to 5°C, a reverse turn is formed around the immunodominant tip (G^5–R^8). Glycosylation on T^{12} 'tightens' the turn slightly as suggested by NOE and CD analysis. In addition, the sugar has a defined conformation with respect to the peptide backbone and influences the local peptide conformation. These data suggest that simple glycosylation may influence the conformational equilibrium of a V3 peptide which contains a domain critical for antibody recognition and virus neutralization. We also show that the ability of cytotoxic T-lymphocytes (CTL) to lyse tumor cells presenting $P18_{IIIB}$ was completely abrogated by threonine glycosylation.**

Key words: NMR; V3 loop; Glycopeptide; CTL

1. Introduction

The envelope glycoprotein (gp120) of human immunodeficiency virus type 1 (HIV-1) is the primary target of the host immune response upon viral infection [1]. The principal neutralizing determinant (PND) has been mapped to the third variable region [2–4] (V3) of the intact protein to which highly effective neutralizing antibodies have been raised [5,6]. However, the search for effective immunotherapies (vaccines) derived from this region of the protein have been hampered by the lack of cross reactivity and viable efficacy of peptide constructs across different viral strains [7,8]. In addition, immunization with gp120 subunit vaccines seem to elicit antibodies which neutralize laboratory-adapted isolates but are ineffective against primary HIV-1 strains [9]. This is due in part to the highly variable nature of the PND sequence between different isolates and the fact that V3, or other more conserved epitopes may be presented differently in vivo as compared with laboratory-adapted isolates. Hence, the discovery of more broadly neutralizing epitopes or a combination of therapeutically useful regimens is a timely concern.

A second structural class of potentially neutralizing targets for immune intervention is the carbohydrate repertoire covalently attached to gp120. The structure and function of these glycan chains have now been studied extensively ([10] and references cited therein), however, the absolute roles of the many sugar chains are still under debate [11]. It has been shown that removal of N-linked glycans from gp120 impairs binding of the protein to $CD4^+$ cells [12]. Infectivity is also decreased when virus is grown in the presence of inhibitors of N-linked glycoprocessing [13]. In addition, synthesis of gp120 in the presence of deoxynorjirimicin affects the functional antigenicity of the V3 loop [14,15]. Recently, the presence of O-linked oligosaccharides on gp120 has been unequivocally determined [16]. Hansen et al. [17] have studied a panel of monoclonal antibodies (MABs) specific for carbohydrate structures and found several to inhibit virus infection in vitro. In particular, those MABs directed to structures such as Tn (α-GalNAc-Ser/Thr), sialosyl-Tn (sialic acid-α-2,6-GalNAc-Ser/Thr), and $Lewis^Y$ antigen (difucosylated lactosamine) blocked infection by cell-free virus of several T-cell lines while also reducing syncytium formation [17]. This raises the possibility that carbohydrate structures on gp120 might constitute a novel immunogenic target for the generation of neutralizing antibodies. Since antibodies to both peptide and sugar epitopes are effective in neutralizing HIV infection, it follows that peptide-carbohydrate conjugates (glycopeptides) may prove to be the actual recognition elements on the protein which elicit the antibody response in vivo. We have begun a program to study the effect that covalently linked carbohydrates have on the three-dimensional conformation of peptides derived from gp120. In this report we compared the structures of a 15-residue peptide from the HIV-1_{IIIB} V3 loop and a glycosylated analogue with *N*-acetylgalactosamine (NAG) α-linked to the threonine four residues to the C-terminal side of the so-called immunodominant tip [18,19] (sequence -GPGR-) of the loop. As this peptide is also an immunodominant epitope for CTL recognition [20–23], we have also tested these peptides for their ability to be recognized by class I-MHC molecule-restricted CTL as measured by lysis of a tumor cell line incubated with the peptides.

2. Materials and methods

2.1. Peptides

The unglycosylated peptide was purchased from Bachem, CA. The glycosylated analogue was prepared by solid-phase synthesis using the Fmoc strategy on an Applied Biosystems peptide synthesizer. Fmoc-protected threonine building block containing a 2,3,4-tri-*O*-acetyl-α-galactosamine was prepared by known methods [24] or was purchased from Oxford Glycosystems Inc. Incorporation of this derivatized residue into the peptide was performed manually by removing the resin

*Corresponding author. NCI/NIH, Bldg 37, Rm 5C02, 37 Convent Dr. MSC 4255, Bethesda, MD 20892-4255, USA. Fax: (1) (301) 402-2275. E-mail: barchi@helix.nih.gov

PII S0014-5793(96)00912-X

and coupling the threonine derivative under Bop activation for 3 h. Cleavage of the peptide from the resin was performed with 95% trifluoroacetic acid (TFA) for 2 h. The precipitated peptide was purified by reverse-phase (C18) HPLC using a gradient of acetonitrile/water each containing 0.05% TFA. The acetate protecting groups on the sugar were removed by brief treatment with freshly prepared 1 M NaOMe in methanol at 0°C. The product was repurified by C18 HPLC affording pure glycosylated peptide as judged by FAB MS and NMR spectroscopy.

2.2. Circular dichroism spectroscopy and FAB mass spectrometry

CD spectra were recorded at room temperature in the wavelength range 190–260 nm, on a Jasco model J-500A/DP501N spectropolarimeter, in Hellma QH cells with a pathlength of 1 mm. Peptide concentrations were 200 μM in 10 mM phosphate buffer, pH 4.8, TFE or TFE/buffer mixtures. Mass spectra were run on a VG-7070-HF instrument using a xenon atom gun and a mixture of DTT/DTE (3:1) in 20% MeOH as the sample matrix.

2.3. NMR spectroscopy

NMR spectroscopy was carried out on a Bruker AMX500 instrument equipped with an inverse, broadband probe. NMR samples were 6 mM ($P18_{IIIB}$) and 10 mM ($P18_{IIIB}$-g) in either 90% H_2O/10% D_2O (DSS as an internal standard) or 100% D_2O. Spectra in 50, 80, or 95% TFE(D_2)/H_2O were also recorded. The pH values of the aqueous samples were adjusted to 4.8 with small amounts of NaOH or HCl solutions and were unbuffered. Spectra were collected at 5, 10 and 25°C under the control of a Eurotherm© variable temperature unit with an accuracy of 0.1°C. Two-dimensional spectra (DQF-COSY [25], TOCSY [26] and NOESY [27]) were recorded employing standard pulse sequences with the number of acquisitions typically set to 64 for the NOESY and DQF-COSY spectra and 32–64 for the TOCSY spectra. Low power presaturation was used to suppress the water resonance during the relaxation delay and the mixing period of the NOESY experiments. In general, spectra were recorded with 2K complex data points in F2 for each of 480–512 t_1 increments with a sweep width of 5050 Hz in each dimension. TOCSY spectra were recorded with an isotropic mixing time of 70 ms and trim pulses of 2.5 ms immediately before and after the spin lock period. NOESY spectra were acquired with mixing times of 200 and 400 ms ($P18_{IIIB}$), or 400 and 500 ms ($P18_{IIIB}$-g). The 400 ms NOESY experiments were used for integration of peak volumes to generate interproton distance constraints. The NOEs were classified into five groups of very strong, strong, medium, weak and very weak (upper bounds set to 2.5, 3.0, 3.5, 4.0 and 5.0 Å), respectively. The lower bound limit was set to 1.9 Å. The temperature coefficients of the amide protons were studied by collecting TOCSY spectra at seven different temperatures between 5 and 35°C in 5 degree increments and are reported in ppb/K. All spectra were processed with UXNMR on an X32 computer or with NMRCOMPASS (Molecular Simulations Inc.) after transfer to a Silicon Graphics Indigo workstation. The data were zero-filled to 1024 points in F1 prior to Fourier transform, multiplied by a shifted (45–60°) sine function and baseline corrected with a polynomial of order 5.

2.4. Molecular modeling and structure calculations

Molecular modeling were performed with the CHARMm 23 [28] force field under the auspices of the QUANTA package (version 4.1) for structure generation and graphics display on a Silicon Graphics Indigo workstation. Models were constructed with the sequence builder facility in QUANTA. The carbohydrate parameters were taken from the POLYSACCHARIDE.RTF residue topology file and linked to the threonine hydroxyl by a PATCH command in CHARMm. Energy minimizations were performed with the Adopted Basis Newton Raphson (ABNR) algorithm. A series of starting structures generated by a minimization-dynamics-minimization protocol were submitted to distance geometry-simulated annealing using X-PLOR [29] with an added potential which accounted for the distance restraints generated from the NOE results. 20 structures with the fewest distance violations and lowest energies were chosen for additional restrained annealing with CHARMm. The starting structures were heated from 0 to 1000 K (10 ps) and slowly cooled over 70 ps (10 ps/100 K) to 300 K and simulated for 50 ps at this temperature while increasing the force constant of the NOE restraints during the cooling

Table 1
^{1}H resonance assignments for the $P18_{IIIB}$ and $P18_{IIIB}$-g in water at pH 4.8

Residue	NH	CαH	CβH	CγH	Others	
Arg-1		4.051 (0.02)[a]	1.906	1.617 (0.02, −0.036)	δCH_2	3.209
					NH	7.272
Ile-2	8.804	4.170	1.799	1.490, 1.186	γCH_3	0.870
					δCH_3	0.850
Gln-3	8.799	4.368	2.055 (−0.028), 1.957	2.332		
Arg-4	8.668	4.387		1.641 (−0.027)	δCH_2	3.162
					NH	7.242
Gly-5	8.520 (−0.016)	4.150, 4.051				
Pro-6		4.447		2.012, 1.971	δCH_2	3.640 (−0.026)
Gly-7	8.642	3.933				
Arg-8	8.305	4.289 (−0.023)	1.779, 1.700	1.561	δCH_2	3.160
					NH	7.217
Ala-9	8.431	4.269 (−0.024)	1.285			
Phe-10	8.342	4.644 (−0.052)	3.103 (−0.032)		2,6H	7.233
			3.004		3,5H	7.339
					4H	7.287
Val-11	8.214 (−0.044)	4.249 (−0.135)	1.996 (−0.034)	0.909 (−0.034)		
Thr-12	8.737 (−0.307)	4.565 (−0.255)	4.249 (−0.157)	1.265 (−0.064)		
Ile-13	8.448	4.170	1.838	1.490, 1.206 (−0.027)	γCH_3	0.949 (−0.052)
					δCH_3	0.850
Gly-14	8.596 (0.052)	4.012 (−0.093), 3.795 (0.124)				
Lys-15	8.152 (−0.153)	4.170	1.818	1.403 (−0.050)	δCH_2	1.693
					εCH_2	2.984 (−0.022)
					εNH_3^+	7.597
GalNAc	1H 4.802	2H 4.081	3H 3.854	4H 3.933	5H	4.012
					$6CH_2$	3.746
					NH	7.873
					CH_3	2.016

[a]Values in parentheses are the differences in chemical shift caused by glycosylation of $P18_{IIIB}$ to $P18_{IIIB}$-g. Negative values refer to upfield shifts.

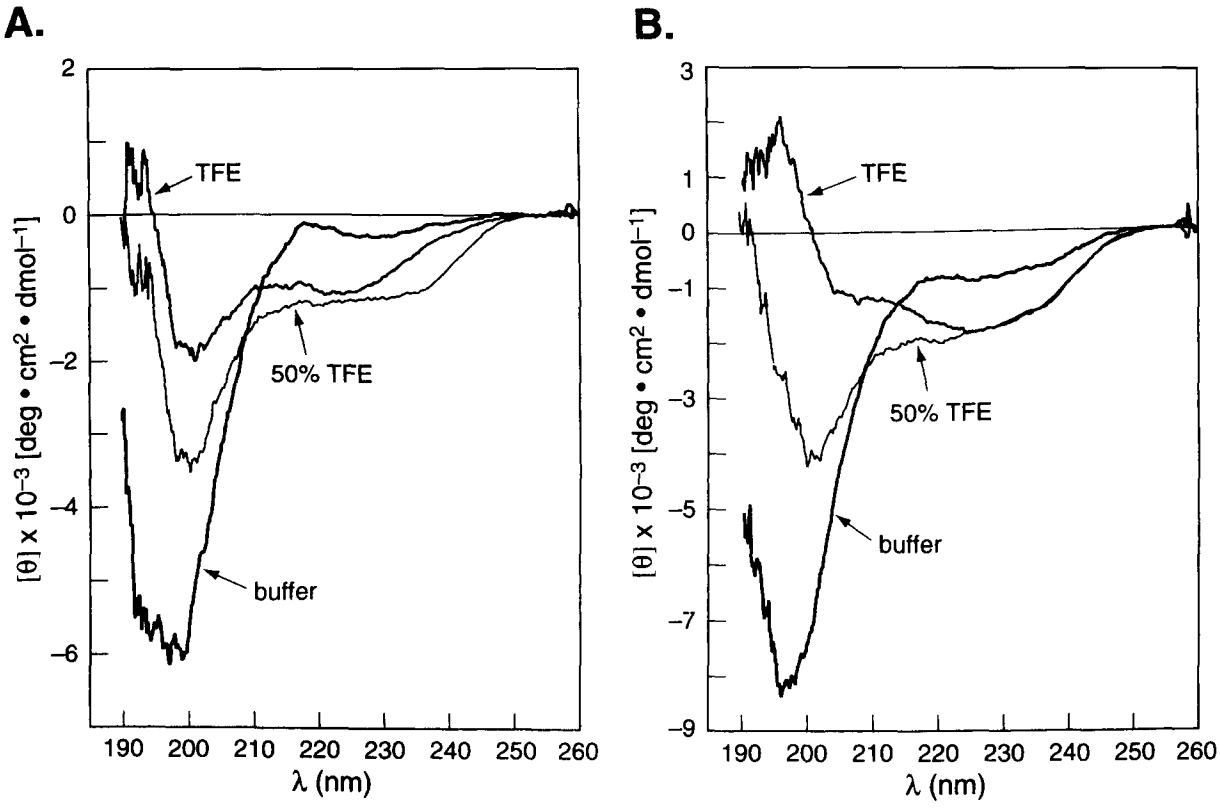

Fig. 1. Circular dichroism spectra of (A) $P18_{IIIB}$ and (B) $P18_{IIIB}$-g in water and TFE mixtures.

period. An additional 50 structures were collected from this step and energy minimized. The procedure was repeated to obtain several final conformers which agreed well with the experimental data.

2.5. CTL assay

The assay and generation of the CTL line utilized here have been previously described [30]. Briefly, target cells (1×10^6) were labeled with 200 μCi of $Na_2{}^{51}CrO_4$ in 200 μl complete medium for 2 h at 37°C. Where appropriate, target cells were pulsed with 1 μM peptides during labeling (a near-saturating concentration). Cells were then washed and added to 96-well plates (2000/well) along with varying amounts of effector cells. After 4 h, supernatants were harvested and counted in an Isomedic gamma counter (ICN). The mean of triplicate samples and percent of ^{51}Cr release were calculated.

3. Results and discussion

The glycopeptide was prepared by solid-phase methods and purified by HPLC. Yields of purified product were greater than 70%. The molecular mass of the synthetic glycopeptide was confirmed by positive ion FAB mass spectrometry. The circular dichroism spectra of $P18_{IIIB}$ and $P18_{IIIB}$-g in phosphate buffer, 50% TFE and 100% TFE are shown in Fig. 1. Both peptides display basically random conformations in phosphate buffer (pH 4.8). As the concentration of TFE is increased, the peptides become more structured as shown by the deviation in the curves to a more positive ellipticity. Slight differences are noticeable between the spectra of the peptide (Fig. 1A) and the glycopeptide (Fig. 1B). In buffer solution the spectra of both samples are similar with the exception of an additional ellipticity at 232 nm in the glycosylated analogue. This region of the spectrum indicates the presence of a bend or turn-type motif [31]. As the lipophilic character of the solvent is increased, this shoulder is consistently larger in the glycosylated analogue.

The ^1H-NMR spectra of $P18_{IIIB}$ and $P18_{IIIB}$-g were recorded at several temperatures but the structurally useful data were obtained at 5–10°C since, for small linear peptides, rapid sampling of conformational substates is reduced at lower temperature. All resonances including the carbohydrate protons for $P18_{IIIB}$-g were completely assigned using standard methods [32]. A comparison of the chemical shifts of both peptides is shown in Table 1. Glycosylation causes a noticeable shift in the δ values only for protons in close proximity to the glycosylated residue (T^{12}). Backbone three-bond proton-proton coupling constants $^3J_{HN,\alpha H}$ measured from the resolution-enhanced, one-dimensional spectra at 5°C revealed values in the intermediate range (6–7.8 Hz) for both peptides suggesting an equilibrium of several conformations even at this low temperature. This trend was further supported by the temperature coefficients of the amide protons determined by a series of TOCSY spectra acquired at seven different temperatures. The temperature coefficient values for $P18_{IIIB}$ spanned from 6.5 to 10.0 ppb/K whereas $P18_{IIIB}$-g values were slightly higher (7.5–13.0 ppb/K). These data indicated that no intramolecular hydrogen bonds normally found in regions of defined secondary structure were evident for either peptide. However, it should be noted that the coefficients for R^8 and V^{11} in $P18_{IIIB}$ (7.3 and 6.5) and in $P18_{IIIB}$-g (7.6 and 7.5) were lower than those for the remaining residues which may indicate that, under the experimental conditions, these residues may participate in forming a more defined structural unit than other segments of the peptide.

The 2D NOESY spectra for each peptide were collected by

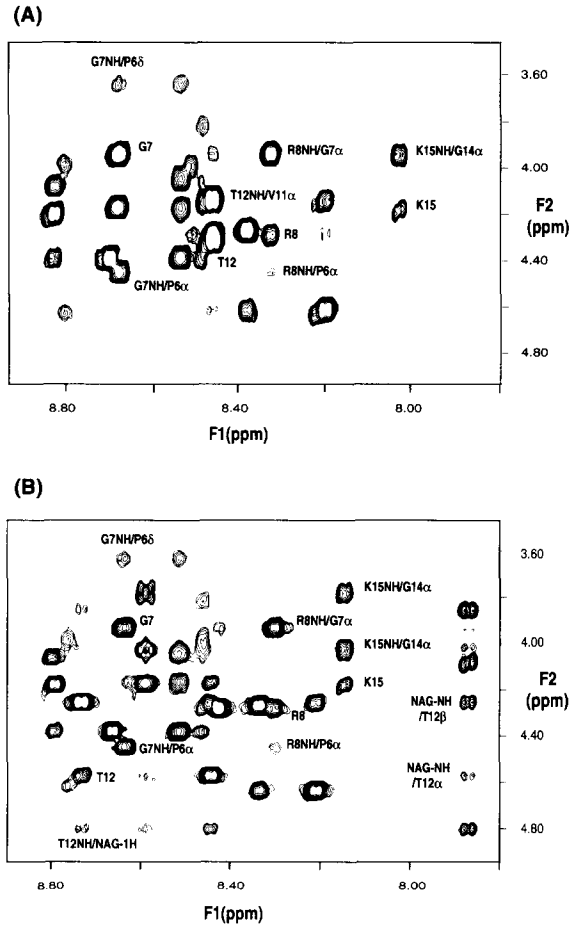

Fig. 2. Comparison of the NH-Hα regions of the NOESY spectra of $P18_{IIIB}$ (A) and $P18_{IIIB}$-g (B). Correlations which describe the turn around G^5–R^8 and that reveal interactions of the NAG-NH with the backbone are labeled.

varying temperature, mixing time and solvent composition. The expanded fingerprint regions from the NOESY spectra of both peptides are compared in Fig. 2. Intraresidue $d_{N\alpha}(i,i)$ and sequential $d_{NN}(i,i+1)$ and $d_{\alpha N}(i,i+1)$ correlations were observed for more than 70% of the residues in both peptides. A schematic diagram of the magnitude of the NOE intensities is shown in Fig. 3. The figure indicates that both $P18_{IIIB}$ and $P18_{IIIB}$-g spectra present weak $d_{\alpha N}(i,i+2)$ correlations between P^6 and R^8 along with strong $d_{NN}(i,i+1)$ (G^7 and R^8) and $d_{N\alpha}(i,i+1)$ (P^6 and G^7) peaks which suggest a type-II β turn is formed in the -GPGR- segment. A very weak NOE interaction between the P^6 δH and the G^7 NH indicates that a small population of a β-I type turn is also present in the conformational equilibrium. The correlations which describe the turn around -GPGR- are absent for $P18_{IIIB}$ at 10°C where they remain visible in the glycosylated analogue. They do appear, however, in the $P18_{IIIB}$ spectra at lower temperatures. A reverse β-turn is therefore observed in both peptides, although this feature is present in a higher proportion of the conformational ensemble sampled by $P18_{IIIB}$-g. These data indicate that in the presence of the sugar this peptide tends toward a more compact structure by tightening the inherent turn centered around -GPGR-. NMR spectra of $P18_{IIIB}$-g were also recorded in different mixtures of water/TFE. At 80% TFE, stronger $d_{NN}(i,i+1)$ peaks and additional $d_{\alpha N}(i,i+2)$ peaks (i.e. A^9/V^{11}, I^{13}/K^{15} and P^6/R^8) were observed. At 95% TFE, the characteristic peaks which define a turn around -GPGR- are more intense under the same conditions, indicating a higher percentage or a tightening of this bend in the structure occurs under lipophilic conditions. The distance data for the remaining backbone in TFE solutions partially resemble a nascent helical form due to strong $d_{NN}(i,i+1)$ and weak $d_{\alpha N}(i,i+2)$ NOEs but no long range $d_{\alpha N}(i,i+3)$ or $d_{\alpha\beta}(i,i+3)$ NOEs were observed. Our data agree with several previous NMR studies [33–35,19] and a crystal structure of a V3 peptide in the presence of an antibody [36] which have described structural elements present in various V3 loop peptides, in particular the highly conserved β-turn around the -GPG(X)- segment.

Several NOEs between the sugar and the peptide backbone were observed as outlined in Table 2. A strong NOE between the T^{12} NH and the NAG NH was detected along with a very strong NOE between the T^{12} βH and NAG H1. In addition, a moderate NOE between NAG H1 and T^{12} γCH_3 along with a strong enhancement between the NAG acetyl methyl group and the amide proton on G^{14} were observed. These NOEs serve to define the preferred torsion angle space sampled by the glycosidic ϕ,ψ angles (ϕ is defined as H1-C1-O1-Thr-Cβ, and ψ as C1-O1-(Thr)-Cβ-Hβ) [37]. When the inter- and in-

Table 2
Peptide-*N*-acetylgalactosamine (NAG) NOEs from $P18_{IIIB}$-g

NAG H	Peptide H	Intensity (calculated distance)
H1	T^{12} NH	very weak (3.84)
	I^{13} NH	weak (3.02)
	G^{14} NH	very weak (3.75)
	T^{12} CH_3	medium (4.2)
	T^{12} αH	very weak (4.02)
	T^{12} βH	very strong (2.2)
H3	T^{12} NH	very weak (3.4)
H5	T^{12} CH_3	strong (3.29)
NH	T^{12} NH	strong (2.75)
	T^{12} αH	very weak (4.6)
	T^{12} βH	medium (3.95)
	T^{12} CH_3	very weak (5.07)
-$COCH_3$	G^{14} NH	strong (3.87)

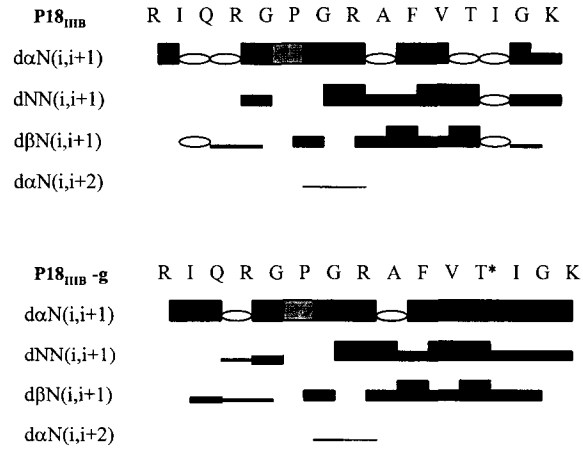

Fig. 3. Amino acid sequence and diagram of NOE connectivities of $P18_{IIIB}$ and $P18_{IIIB}$-g collected at 278 K. The thickness of the bars directly correlates with the strength of the NOE crosspeak. A blank circle represents an NOE of unknown intensity due to peak overlap.

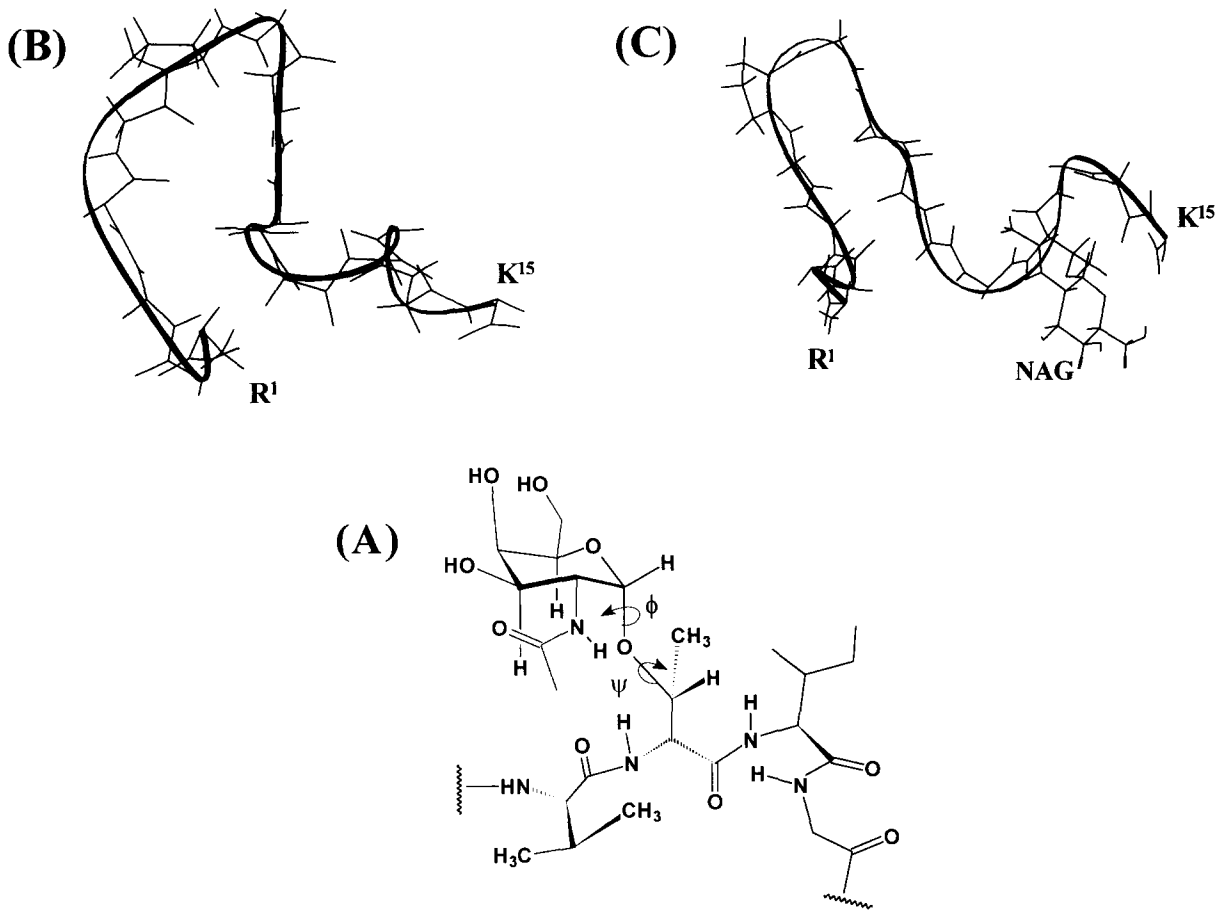

Fig. 4. (A) Model of the glycosylated residue T^{12} and the relationship of the sugar with the surrounding amino acid sequence based on the NOEs in Table 2. The definitions of angles ϕ and ψ are shown. (B,C) Representative structures from the molecular dynamics calculations of $P18_{IIIB}$ and $P18_{IIIB}$-g, respectively. The depiction in (C) represents the trajectory which best fits the data that derived the model of the segment shown in (A).

traresidue correlations in this portion of the peptide are included (see Fig. 3), a reasonable description of this segment may be ascertained. A representation of a model derived from these data for the conformation of the NAG with respect to the surrounding peptide sequence is shown in Fig. 4A.

This structural prediction was also borne out in the calculations using a simulated annealing-molecular dynamics protocol. Fig. 4B and C depict low energy models derived from the structure calculations (as described in Section 2.4) for $P18_{IIIB}$ and $P18_{IIIB}$-g, respectively. Not surprisingly, the calculations yielded several families of conformations for both peptides due to the paucity of interresidue restraints and the inherent flexibility for peptides of this size. However, a reasonably defined conformation was found for the -GPGR- segment as demonstrated by the RMSD values in this region. The entire backbone RMSD was 3.7 Å for $P18_{IIIB}$ but only 0.9 Å for the residues G^5–R^8. Glycosylation of T^{12} not only decreased the RMSD value of the backbone atoms to 2.7 Å, but also decreased the value for the G^5–R^8 segment from 0.9 to 0.6 Å. In addition, the RMSD value for residues V^{11}–I^{13} was 1.0 Å for $P18_{IIIB}$ and 0.4 Å for $P18_{IIIB}$-g calculated for all heavy atoms (excluding the NAG atoms) in this segment. A survey of the best-fit calculated structures suggested the optimum ranges for the ϕ and ψ glycosidic torsions were between -53 and $-25°$, and -4 and 40°, respectively. Therefore, although the peptides sample several different conformers even at low temperature, the presence of the sugar imparts additional structural integrity to the residues immediately flanking the glycosylated amino acid. In addition, the reverse turn encompassing -GPGR- is populated to a slightly higher extent for $P18_{IIIB}$-g than in $P18_{IIIB}$. The explanation for this phenomenon is not immediately evident. Stabilization of a β-turn in the immediate vicinity of the glycosylated residue has been documented for N- [38] and O-linked [39] glycopeptides. However, upstream effects such as the one described here are not as common [40]. It is possible the local restriction on the conformation near the sugar transmits an effect to distant, defined structural elements in the peptide, such as the β-turn around the highly conserved -GPG- sequence. As shown here, however, it is still difficult to firmly establish defined structural features on small, linear peptides. The use of longer sequences, higher-order oligosaccharides and/or additional molecular constraints may advance this conceptual approach of structural 'tuning' via glycosylation. A very recent NMR study [41] showed that the -GPG(X)-β-turn was conserved in peptides with a β-glucosamine covalently attached to N^{306} near the N-terminal side of different V3 loop sequences.

The $P18_{IIIB}$ sequence has been shown to contain an epitope recognized by $CD8^+$ D^d class I MHC-restricted murine CTL [20]. These CTL effectively lyse a target D^d positive cell line

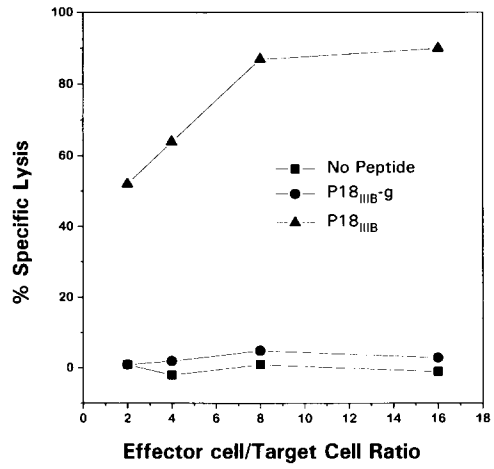

Fig. 5. CTL specific for the sequence RGPGRAFVTI presented by the murine class I molecule D^d recognize target cells pulsed with 1 μM $P18_{IIIB}$ (▲) but not 1 μM $P18_{IIIB}$-g (●). Target cells without peptide (■) are also not recognized. Target cells were from the D^d positive mastocytoma cell line P815 (see Section 2).

either expressing HIV-1_{IIIB} gp160 endogenously or pulsed with $P18_{IIIB}$. It was later determined [42–44] that the minimum sequence necessary is actually a 10-mer peptide RGPGRAFVTI. The ability of $P18_{IIIB}$-g to sensitize D^d-bearing target cells for lysis by these CTL specific for this 10-mer sequence was tested in a ^{51}Cr release assay. Fig. 5 shows that $P18_{IIIB}$ pulsed targets are almost completely killed at high effector/target cell ratios, whereas $P18_{IIIB}$-g pulsed targets are not killed above background. This is most probably due to undesired steric effects where the sugar essentially destroys the high affinity binding interaction between the glycopeptide and either MHC-I molecules or the T-cell receptor on the target cells. Alternatively, the modified peptide may not present conformations in the vicinity of the carbohydrate which are recognized by its binding partners. Since previous data indicated [21–23,44] that V^{11} was critical for $P18_{IIIB}$ binding to the target T-cell receptor, and that T^{12} contacted the T-cell receptor as well, this binding event is more likely to be adversely effected by T^{12} glycosylation.

In conclusion, the solution conformation of a 15-residue peptide, O-glycosylated at Thr-12 with an α-linked galactosamine, was shown to be quite different from the unglycosylated sequence. The highly conserved turn motif (-GPGR-), as determined from structural studies on other V3 peptides, is present in both peptides at low temperature and sampled to a higher extent in the glycosylated analogue. The ability of this peptide to sensitize tumor targets for specific MHC-I-restricted T-cell lysis, was abolished upon T^{12} glycosylation. Studies on the structure-activity relationships of other glycosylated gp120 peptides with respect to their immunogenicity are in progress.

Acknowledgements: The authors would like to thank Kazuyasu Sakaguchi, Laboratory of Cell Biology, National Cancer Institute, for help in preparing $P18_{IIIB}$-g. We also thank Dr. Peter Roller, Laboratory of Medicinal Chemistry, for running the CD spectra. This work was supported by the AIDS Targeted Antiviral Program of the Office of the Director of the National Institutes of Health (X.H. and J.J.B. Jr.).

References

[1] Gorny, M.K., Xu, J.Y., Karwowska, S., Buchbinder, A. and Zolla-Pazner, S. (1993) J. Immunol. 150, 635–643.
[2] Javaherian, K., Langlois, A.J., McDanal, C., Ross, K.L., Eckler, L.I., Jellis, C.L., Profy, A.T., Rusche, J.R., Bolognesi, D.P., Putney, S.D. and Matthews, T.J. (1989) Proc. Natl. Acad. Sci. USA 86, 6768–6772.
[3] Goudsmit, J., Debouck, C., Meloen, R.H., Smit, L., Bakker, M., Asher, D.M., Wolff, A., Gibbs, C.J., Jr. and Gajdusek, D.C. (1988) Proc. Natl. Acad. Sci. USA 85, 4478–4482.
[4] Palker, T.J., Clark, M.E., Langlois, A.J. Matthews, T.J., Weinhold, K.J., Randall, R.R., Bolognesi, D.P. and Haynes, B.F. (1988) Proc. Natl. Acad. Sci. USA 85, 1932–1936
[5] Rusche, J.R., Javaherian, K., McDanal, C., Petro, J., Lynn, D.L., Grimaila, R., Langlois, A.J., Gallo, R.C., Arthur, L.O., Fischinger P.J., Bolognesi, D.P., Putney, S.D. and Matthews, T.J. (1988) Proc. Natl. Acad. Sci. USA 85, 3198–3202
[6] White-Scharf, M.E, Potts, B.J., Smith, L.M., Sokolowski, K.A., Rusche, J.R. and Silver, S. (1993) Virology 192, 197–206
[7] Fast, P.E. and Walker, M.C. (1993) AIDS 7 (Suppl. 1), S147–159.
[8] Steimer, K.S., Sakamoto, D., Sun, Y.D., West, D., Baenziger, J. and Sinangil, F. (1994) J. Cell. Biochem. 8B, 114.
[9] Mascola, J.R., Snyder, S.W., Weislow, O.S., et al. (1996) J. Infect. Dis. 173, 340–348.
[10] Feizi, T. and Larkin, M. (1990) Glycobiology, 1, 17–23.
[11] Fenouillet, E., Gluckman, J.C. and Jones, I.M. (1994) Trends Biochem. Sci. 19, 65–70.
[12] Matthews, T.J., Weinhold, K.J., Lyerly, H.K., Langlois, A.J., Wigzell, H. and Bolognesi, D.P. (1987) Proc. Natl. Acad. Sci. USA 84, 5424–5428.
[13] Dedera, D., Vander Heyden, N. and Ratner, L. (1990) AIDS Res. Hum. Retroviruses 6, 785–794.
[14] Fenouillet, E. and Gluckman, J.C. (1991) J. Gen. Virol. 72, 1919–1926.
[15] Jones, I. and Jacob, G.S. (1991) Nature 352, 198.
[16] Bernstein, H.B., Yucker, S.P., Huner, E., Schutzbach, J.S. and Compans, R.W. (1994) J. Virol. 68, 463–468.
[17] Hansen, J.-E.S., Clausen, H. Nielsen, C., Teglbjærg, L.S., Hansen, L.L., Nielsen, C.M., Dabelsteen, E., Mathiesen, L., Hakomori, S.-I. and Nielsen, J.O. (1990) J. Virol. 64, 2833–2840.
[18] Gupta, G., Anantharamaiah, G.M., Scott, D.R., Eldrige, J.H. and Meyers, G. (1993) J. Biomol. Struct. Dyn. 11, 345–366.
[19] Fontenot, J.D., Gatewood, J.M., Santhana Mariappan, S.V., Pau, C.-P., Parekh, B.S., George, J.R. and Gupta, G. (1995) Proc. Natl. Acad. Sci. USA 92, 315–319.
[20] Takahashi, H., Cohen, J., Hosmalin, A., Cease, K., Houghten, R., Cornette, J.L., Delisi, C., Moss, B., Germain, R.N. and Berzofsky, J.A. (1988) Proc. Natl. Acad. Sci. USA 85, 3105–3109
[21] Takahashi, H., Houghten, R, Putney, S.D., Margulies, D.H., Moss, B., Germain, R.N. and Berzofsky, J.A. (1989) J. Exp. Med. 170, 2023–2035.
[22] Takahashi, H., Merli, S., Putney, S.D., Houghten, R., Moss, B., Germain, R.N. and Berzofsky, J.A. (1989) Science 246, 118–121.
[23] Takahashi, H., Nakagawa, Y., Pendleton, C.D., Houghten, R., Yokomuro, K., Germain, R.N. and Germain, R.N. (1992) Science 255, 333–336.
[24] Lüning, B.Norberg, T. and Tejbrant, J. (1989) Glycoconj. J. 6, 5–19.
[25] Rance, M., Sorenson, O.W., Bodenhausen, G., Wagner, G., Ernst, R.R. and Wüthrich, K. (1983) Biochem. Biophys. Res. Commun. 117, 479–485.
[26] Bax, A. and Davis, D.G. (1985) J. Magn. Reson. 65, 355–360.
[27] Macura S. and Ernst, R.R. (1980) Mol. Phys. 41, 95–117.
[28] Brooks, B.R., Bruccoleri, R.E., Olafson, B.D., States, D.J., Swaminathan, S. and Karplus, M. (1983) J. Comput. Chem. 4, 187–217.
[29] Brüenger, A.T. (1993) X-PLOR v. 3.1: A System for X-ray Crystallography and NMR, Yale University Press, New Haven.
[30] Alexander-Miller, M.A., Leggatt, G.R. and Berzofsky, J.A. (1996) Proc. Natl. Acad. Sci. USA 93, 4102–4107.
[31] Woody, R.W. (1995) Methods Enzymol. 246, 34–71.
[32] Wüthrich, K. (1986) NMR of Proteins and Nucleic Acids, Wiley, New York.

[33] Chandrasekhar, K., Profy, A.T. and Dyson, H.J. (1991) Biochemistry 30, 9187–9194.
[34] Zvi, A., Kustanovich, I., Hayek, Y., Matsushita, S. and Anglister, J. (1995) FEBS Lett. 368, 267–270
[35] De Lorimier, R., Moody, M.A., Haynes, B.F. and Spicer, L.D. (1994) Biochemistry 33, 2055–2062.
[36] Rini, J.M., Stanfield, R.L., Stura, E.A., Salinas, P.A., Profy, A.T. and Wilson, I.A. (1993) Proc. Natl. Acad. Sci. USA 90, 635–6329
[37] Vliegenthart, J.F.G., Dorland, L. and Van Halbeek, H. (1983) Adv. Carbohydr. Chem. Biochem. 41, 209–374.
[38] Imperiali, B. and Rickert, K.W. (1995) Proc. Natl. Acad. Sci. USA 92, 97–101.
[39] Urge, L., Gorbics, L. and Otvos, Jr., L. (1992) Biochem. Biophys. Res. Commun. 184, 1125–1132.
[40] Gerken, T.A., Butenhof, K.J. and Shogren, R. (1989) Biochemistry, 28, 5536–5543.
[41] Markert, R.L.M., Ruppach, H., Gehring, S., Dietrich, U., Mierke, D.F., Kock, M., RubsamenWaigmann, H. and Griesinger, C. (1996) Eur. J. Biochem. 237, 188–204.
[42] Shirai, M., Pendleton, C.D. and Berzofsky, J.A. (1992) J. Immunol. 148, 1657–1667.
[43] Kozlowski, S., Corr, M., Takeshita, T., Boyd, L.F., Pendleton, C.D., Germain, R.N., Berzofsky, J.A. and Margulies, D.H. (1992) J. Exp. Med. 175, 1417–1422.
[44] Takeshita, T., Takahashi, H., Kozlowski, S., Ahlers, J.D., Pendleton, C.D., Moore, R.L., Nakagawa, Y., Yokomura, K., Fox, B.S., Margulies, D.H. and Berzofsky, J.A. (1995) J. Immunol. 154, 1973–1986.